Manipulation of the Steering and Shaping of SPPs via Spatially Inhomogeneous Polarized Illumination

Tzu-Hsiang Lan[1] and Chung-Hao Tien[2,*]

[1]*Department of Photonics and Institute of Electro-optical Engineering, National Chiao Tung University, Hsinchu 30010, Taiwan*
[2]*Department of Photonics and Display Institute, National Chiao Tung University, Hsinchu 30010, Taiwan.*
**chtien@mail.nctu.edu.tw*

Abstract: In this paper, we demonstrated a far-field scheme for the manipulation of locally excited surface plasmon polaritons (SPPs). This scheme features steering and shaping capabilities, and relies on the focusing of a high numerical aperture, in conjunction with spatially inhomogeneous polarized (SIP) illumination. We were able to control the propagation and direction of SPPs, via the field distribution of polarization at the entrance pupil, without the need for an aperture, protrusion or any other near-field features. Depending on the axial position of the focus, the field distribution of excited SPPs revealed either counter-propagating interference or a multi-casting plasmonic source. The results of near-field imaging demonstrated the versatility of the SPPs, showing strong agreement with the predictions made during simulations. Due to the simplicity and versatility of the proposed method, we believe that it could have a significant impact the processes employed in the excitation of a variety of SPPs.

OCIS codes: (050.1960) Diffraction theory; (180.4243) Near-field microscopy; (240.6680) Surface plasmons; (260.5430) Polarization.

References and links

1. H. Raether, "Surface-plasmons on smooth and rough surfaces and on gratings," Springer Tracts Mod. Phys. **111**, 1–133 (1988).
2. S. A. Maier, *Plasmonics: Fundamentals and Applications* (Springer, 2007).
3. S. I. Bozhevolnyi, and F. A. Pudonin, "Two-dimensional micro-optics of surface plasmons," Phys. Rev. Lett. **78**(14), 2823–2826 (1997).
4. F. I. Baida, D. Van Labeke, A. Bouhelier, T. Huser, and D. W. Pohl, "Propagation and diffraction of locally excited surface plasmons," J. Opt. Soc. Am. A **18**(7), 1552–1561 (2001).
5. W. L. Barnes, A. Dereux, and T. W. Ebbesen, "Surface plasmon subwavelength optics," Nature **424**(6950), 824–830 (2003).
6. M. I. Stockman, "Nanofocusing of optical energy in tapered plasmonic waveguides," Phys. Rev. Lett. **93**(13), 137404 (2004).
7. H. Ditlbacher, J. R. Krenn, G. Schider, A. Leitner, and F. R. Aussenegg, "Two-dimensional optics with surface plasmon polaritons," Appl. Phys. Lett. **81**(10), 1762–1764 (2002).
8. L. L. Yin, V. K. Vlasko-Vlasov, J. Pearson, J. M. Hiller, J. Hua, U. Welp, D. E. Brown, and C. W. Kimball, "Subwavelength focusing and guiding of surface plasmons," Nano Lett. **5**(7), 1399–1402 (2005).
9. A. G. Curto, and F. J. G. Abajo, "Near-field optical phase antennas for long-range plasmon coupling," Nano Lett. **8**(8), 2479–2484 (2008).
10. B. Hecht, H. Bielefeldt, L. Novotny, Y. Inouye, and D. W. Pohl, "Local excitation, scattering, and interference of surface plasmons," Phys. Rev. Lett. **77**(9), 1889–1892 (1996).
11. Q. W. Zhan, "Evanescent Bessel beam generation via surface plasmon resonance excitation by a radially polarized beam," Opt. Lett. **31**(11), 1726–1728 (2006).
12. W. B. Chen, and Q. W. Zhan, "Realization of an evanescent Bessel beam via surface plasmon interference excited by a radially polarized beam," Opt. Lett. **34**(6), 722–724 (2009).
13. Z. J. Hu, P. S. Tan, S. W. Zhu, and X. C. Yuan, "Structured light for focusing surface plasmon polaritons," Opt. Express **18**(10), 10864–10870 (2010).

#133327 - $15.00 USD Received 18 Aug 2010; revised 4 Oct 2010; accepted 13 Oct 2010; published 20 Oct 2010

14. T. Grosjean, S. S. Saleh, M. A. Suarez, I. A. Ibrahim, V. Piquerey, D. Charraut, and P. Sandoz, "Fiber microaxicons fabricated by a polishing technique for the generation of Bessel-like beams," Appl. Opt. **46**(33), 8061–8067 (2007).
15. B. H. Jia, X. S. Gan, and M. Gu, "Direct measurement of a radially polarized focused evanescent field facilitated by a single LCD," Opt. Express **13**(18), 6821–6827 (2005).
16. N. Passilly, R. de Saint Denis, K. Aït-Ameur, F. Treussart, R. Hierle, and J. F. O. Roch, "Simple interferometric technique for generation of a radially polarized light beam," J. Opt. Soc. Am. A **22**(5), 984–991 (2005).
17. V. G. Niziev, R. S. Chang, and A. V. Nesterov, "Generation of inhomogeneously polarized laser beams by use of a Sagnac interferometer," Appl. Opt. **45**(33), 8393–8399 (2006).
18. I. Iglesias, and B. Vohnsen, "Polarization structuring for focal volume shaping in high-resolution microscopy," Opt. Commun. **271**(1), 40–47 (2007).
19. A. K. Spilman, and T. G. Brown, "Stress birefringent, space-variant wave plates for vortex illumination," Appl. Opt. **46**(1), 61–66 (2007).
20. L. Z. Rao, J. X. Pu, Z. Y. Chen, and P. Yei, "Focus shaping of cylindrically polarized vortex beams by a high numerical-aperture lens," Opt. Laser Technol. **41**, 241–246 (2009).
21. D. Kalaidji, M. Spajer, N. Marthouret, and T. Grosjean, "Radially polarized conical beam from an embedded etched fiber," Opt. Lett. **34**(12), 1780–1782 (2009).
22. M. G. Somekh, G. Stabler, S. G. Liu, J. Zhang, and C. W. See, "Wide-field high-resolution surface-plasmon interference microscopy," Opt. Lett. **34**(20), 3110–3112 (2009).
23. T. Wilson, R. Juskaitis, and P. Higdon, "The imaging of dielectric point scatterers in conventional and confocal polarisation microscopes," Opt. Commun. **141**(5-6), 298–313 (1997).
24. L. Novotny, and B. Hecht, "Principles of Nano-optics," (Cambridge U. Press, 2006).
25. P. Török, P. Varga, and G. R. Booker, "Electromagnetic diffraction of light focused through a planar interface between materials of mismatched refractive-indexes - structure of the electromagnetic-field. 1," J. Opt. Soc. Am. A **12**(10), 2136–2144 (1995).
26. E. Wolf, "Electromagnetic Diffraction in Optical Systems. I. An Integral Representation of the Image Field," Proc. R. Soc. Lond. A Math. Phys. Sci. **253**(1274), 349–357 (1959).
27. B. Richards, and E. Wolf, "Electromagnetic Diffraction in Optical Systems. II. Structure of the Image Field in an Aplanatic System," Proc. R. Soc. Lond. A Math. Phys. Sci. **253**(1274), 358–379 (1959).
28. M. Mansuripur, "Certain computational aspects of vector diffraction problems," J. Opt. Soc. Am. A **6**(6), 786–805 (1989).
29. A. Bouhelier, F. Ignatovich, A. Bruyant, C. Huang, G. Colas des Francs, J. C. Weeber, A. Dereux, G. P. Wiederrecht, and L. Novotny, "Surface plasmon interference excited by tightly focused laser beams," Opt. Lett. **32**(17), 2535–2537 (2007).
30. T. Grosjean, F. Baida, and D. Courjon, "Conical optics: the solution to confine light," Appl. Opt. **46**(11), 1994–2000 (2007).
31. H. Kano, S. Mizuguchi, and S. Kawata, "Excitation of surface-plasmon polaritons by a focused laser beam," J. Opt. Soc. Am. B **15**(4), 1381–1386 (1998).
32. P. S. Tan, X. C. Yuan, J. Lin, Q. Wang, and R. E. Burge, "Analysis of surface plasmon interference pattern formed by optical vortex beams," Opt. Express **16**(22), 18451–18456 (2008).
33. P. S. Tan, X. C. Yuan, J. Lin, Q. Wang, T. Mei, R. E. Burge, and G. G. Mu, "Surface plasmon polaritons generated by optical vortex beams," Appl. Phys. Lett. **92**(11), 3 (2008).
34. A. Bouhelier, and G. P. Wiederrecht, "Surface plasmon rainbow jets," Opt. Lett. **30**(8), 884–886 (2005).
35. M. F. Xiao, R. Machorro, and J. Siqueiros, "Interference in far-field radiation of two contra-propagating surface plasmon polaritons in the Kretchmann configuration," J. Vac. Sci. Technol. A **16**(3), 1420–1424 (1998).
36. D. Van Labeke, and D. Barchiesi, "Probes for scanning tunneling optical microscopy - a theoretical comparison," J. Opt. Soc. Am. A **10**(10), 2193–2201 (1993).

1. Introduction

Recently, there has been a surge of interest in the characteristics of electromagnetic modes supported by a variety of thin film structures, in both the fundamental and applied sciences. A great deal of attention has been devoted to surface plasmon polaritons (SPPs), which are confined to the metal-dielectric interface; exponentially decaying as they move away from the interface into the neighboring media. The excitation of SPPs in metallic films with complex permittivity $\varepsilon_m(\omega) = \varepsilon_m'(\omega) + i\varepsilon_m''(\omega)$ is determined by the law of dispersion that imposes a narrow set of resonant angular vectors at a given frequency of excitation [1,2]. Because the relationship between the excitation and dispersion of SPPs is related to the characteristics of the adjacent dielectric material, a great number of SPP-based modulators and switches have been developed over the last few years [3–7]. Due to the unique behavior of SPPs in the near-field, researchers have recently shifted their attention to the focus and guidance of SPPs. In the journal NANO Letters of a 2005 study, Yin et al. reported a method for launching and

#133327 - $15.00 USD Received 18 Aug 2010; revised 4 Oct 2010; accepted 13 Oct 2010; published 20 Oct 2010

focusing SPPs through a strip waveguide, utilizing subwavelength hole as a dipole source of SPPs [8]. In addition, Alberto et al. introduced phase delay into the arrangement of the array of holes, creating a so-called "near-field optical phase antenna" to refocus the source of the SPPs [9]. However, the design and implementation of surface-feature-mediated long-range plasmon were extremely delicate in the near-field, which unavoidably increased the difficulties in practical implementation.

Localized optical field engineering is complementary to near-field engineering, but offers significant advantages in its approach to excitation, thanks to the wide spectrum of wave vectors it provides. Many studies utilize a high-numerical-aperture (NA) objective lens to tightly focus laser beams and precisely control the excitation of SPPs on a structureless metal surface [10,11]. Based on the collinear Kretchmann setup, Q. Zhan focused radial polarization on a dielectric/metal interface. Owing to the fact that the entire beam was p-polarized (TM-polarized) with respect to the incidence plane of the multilayer structure, the subwavelength Bessel beam was subject to resonant conditions and could be regarded as an SPPs point source [11,12]. In addition, modified radial polarization with a cogwheel-like light source, was also adapted to symmetrically focus SPPs [13]. According to previous studies, most of the generated SPPs were center-symmetric and identical to the focus field of the longitudinal component. Alternatives for the generation of asymmetrical SPPs and their properties have not been adequately reported or discussed; which has hindered advancement in the application of SPPs.

In this study, we have maintained our commitment to far-field schemes, in proposing a flexible new approach to launching SPPs, with versatile field distribution. This method is based on a collinear configuration, in conjunction with spatially inhomogeneous polarized (SIP) illumination [14–21]. The structure of the polarization for the SIP beam at the pupil entrance fulfills a similar function to the array of holes used in near-field engineering. This enables a variety of SPPs, due to the three-dimensional characteristics of the optical field. To elaborate on the underlying physics and mechanisms, we produced a phenomenology model associated with the manipulation of SPPs on a flat metallic surface. In addition, we verified the proposed scheme through observation of experiments and finite-difference time-domain (FDTD) simulation.

2. Optical configuration

We employed wide field SPR microscopy [11–13,22], illuminated by a specific state of polarization, as illustrated in Fig. 1(a). The total internal reflection (TIR) objective with gold coated cover glass was used to replace the conventional prism coupler, as in a collinear Kretchmann setup. The cover glass was coated with 40 nm of Au ($n = 0.203 + 3.105i$ at $\lambda_0 = 632.8$ nm). The gap between the objective (Olympus 60x NA = 1.45) and the cover glass was filled with oil, with a matching liquid refractive index. The light source was created to perform a specific state of polarization, a so-called SIP beam, as shown in Fig. 1(b). The SIP beam comprised two orthogonal components: radial and azimuthal polarizations. The spatial arrangement of the polarizing structure on the plane of the pupil was directly related, to the three-dimensional optical field in the focal region of the high-NA lens, by a simple real-valued geometry-dependent matrix [23].

As longitudinal electric oscillation waves, the SPPs followed only the direction of the electric field induced by the radially polarized focus. In contrast, the azimuthal polarization imposed none of the resonant in-plane angular vectors, with no excitation of SPPs. The ability to alter the properties and subsequent polarization arrangement at the entrance pupil offered a simple but effective SPP launching scheme, with respect to individual incident planes. The polarization distribution at the entrance pupil was characterized by three parameters: $\delta\phi$, ϕ_0 and $\Delta\phi$, as shown in Fig. 1(b). $\delta\phi$ is the size of the TM-polarized sector at the entrance pupil. ϕ_0 is the center of angular arc of TM-polarized sector determining the direction guiding the

#133327 - $15.00 USD Received 18 Aug 2010; revised 4 Oct 2010; accepted 13 Oct 2010; published 20 Oct 2010

launched plasmonic wave. $\Delta\Phi$ represents the angular distance between two TM-polarized sectors.

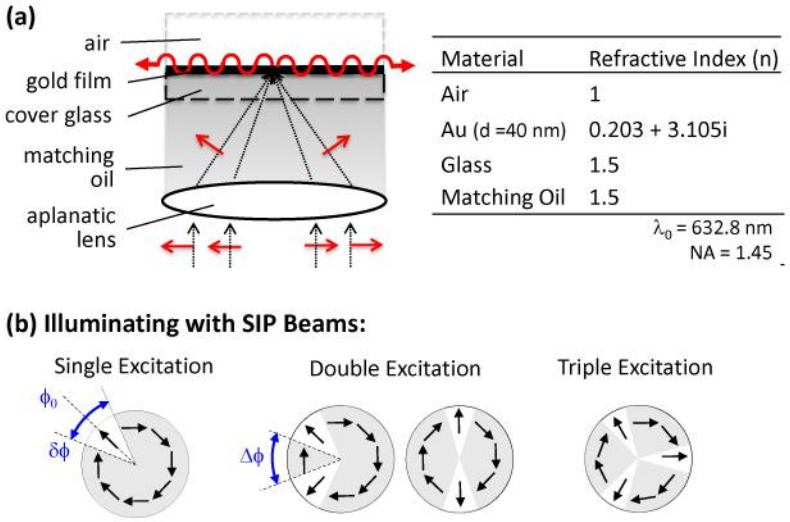

Fig. 1. A schematic diagram of the optical setup for steering and shaping SPPs, utilizing spatially inhomogeneous polarized (SIP) illumination. The table [right side of Fig. 1(a)] shows the parameters of the proposed optical setup with a working wavelength of λ_0 = 632.8 nm. The SIP beams were grouped into three schemes [Fig. 1(b)]: single, double and triple excitation, respectively. Three parameters were adjusted to identify the character of the features of SIP beams; where $\delta\phi$ represents the size of the TM-polarized sector at the pupil entrance, ϕ_0 is the center of angular arc of TM-polarized sector, and $\Delta\phi$ represents the angular distance between two TM-polarized sectors.

In the past, the study of field-distribution of focus excited SPPs was well developed through the use of vectorial Debye integral of Richards and Wolf, in conjunction with Fresnel transmission coefficients of a dielectric/metal/air structure [24–28]. Several researchers adapted this method of calculation to study the behavior of SPPs, under various degrees of illumination [11,29–34]. The state of polarization at the pupil entrance determined the field distribution at the focal point, which could be calculated by means of vectorial calculation. When angular contribution was restricted to a narrow band, the field distribution of the SPPs was proportional to the longitudinal component of the focus. Integral equations with embedded Fresnel transmission coefficients could be used to describe the excitation of the SPPs. However, the quantitative description and analytical solution mentioned above are valid only for symmetrically focus excited SPPs. Under the conditions of our method, when illumination is an SIP beam, rather than conventional polarization, the result of the excited SPPs indicates more than simple constructive or destructive interference. This discussion would be incomplete without considering the propagational behavior of plasmonic waves when the structured illumination contained attributes of asymmetrically-distributed polarization. For example, in the case of a single excitation, the field distribution of SPPs would show a discrepancy between the results of the experiment and the outcome of the vectorial Debye integral. This is because conventional models are unable to describe the coma-shaped field distribution of SPPs, in which their propagating nature is revealed. We have improved on previous versions and propose a new phenomenological model associated with a semi-quantitative description, to illustrate the mechanism of SPP generation and its underlying physics. A schematic diagram is illustrated in Fig. 2.

#133327 - $15.00 USD Received 18 Aug 2010; revised 4 Oct 2010; accepted 13 Oct 2010; published 20 Oct 2010

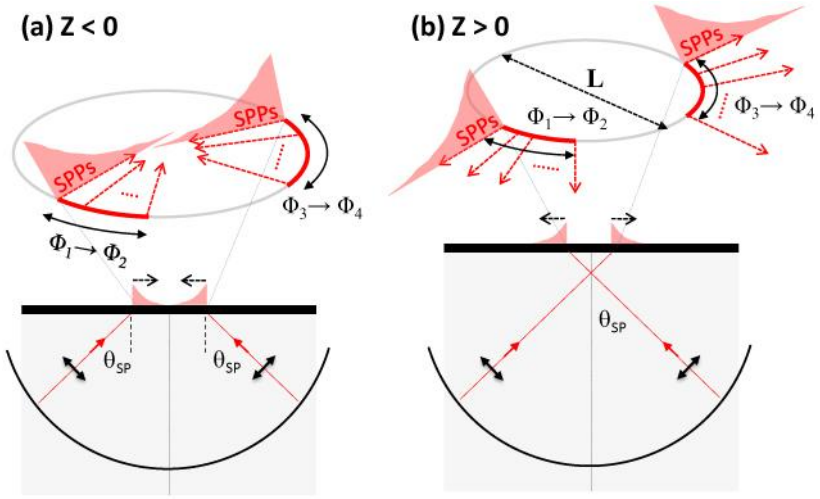

Fig. 2. A schematic diagram of the mechanism used to generate surface plasmon waves originating from a virtual annular ring via spatially inhomogeneous polarized beams. The virtual annular ring is the cross section between the light cone and the observation plane, and it consists of red and gray arcs which indicate the positions of TM- or TE-polarized rays impinged, respectively.

From the viewpoint of geometric projection, we treated SIP beam as a group of rays propagating along its Poynting vector toward the vicinity of focus due to the guidance of the lens. Each ray carried either TM- or TE-polarization depending on its emitting position at entrance pupil, and only TM-polarized ray could effectively excited SPPs. Because of phase matching condition, contributed rays were restricted to a light cone with a narrow bandwidth. The cross section between the light cone and the observation plane pointed out a virtual annular ring. This virtual annular ring was the connection of each exciting positions of SPPs and its diameter was highly relevant to the position of focus. In other word, the polarization structure of the SIP beam at the pupil entrance determined the pattern of SPP excited position which fulfilled a similar function to the array of holes used in near-field engineering.

In this paper, we have presented an alternative to bringing partial in-plane wave vectors to create specific conditions for the excitation of SPPs located on the virtual annular ring, by switching the state of polarization between TM and TE modes. The characteristic of virtual annular ring fulfills a similar function to the array of holes used in near-field engineering. As shown in the Fig. 2, the gray circle with diameter L represents the virtual annular ring. The red arcs indicate the active regions where the SPPs are launched; also they are the projection of TM-polarized sectors of SIP beam at the entrance pupil.

As the metallic film was below the focus (Z < 0), the plasmon waves counter propagated toward the center to interfere mutually. As the metallic film is above the focus (Z > 0), the plasmon waves propagated away from the center, effectively casting multiple plasmonic waves. Under these conditions, no interference occurred within the virtual annular ring. The overall behavior of launched SPPs could be described as a summation of individual plasmon waves resembling a secondary source originating from the virtual annular ring, as shown in Eq. (1).

$$E_{total}(r,\varphi) = \int_{\Phi_1}^{\Phi_2} \frac{dE_{SP}(\varphi)}{d\varphi} d\varphi + \int_{\Phi_3}^{\Phi_4} \frac{dE_{SP}(\varphi)}{d\varphi} d\varphi + \ldots \tag{1}$$

and

$$E_{SP}(r,\varphi) = E_0(r,\varphi) e^{-\alpha d(\varphi,L)} e^{i\beta d(\varphi,L)} \tag{2}$$

$$d(\varphi,\mathrm{L}) = L - r\cos(\varphi - \varphi_0) \tag{3}$$

#133327 - $15.00 USD Received 18 Aug 2010; revised 4 Oct 2010; accepted 13 Oct 2010; published 20 Oct 2010

where r and ϕ refer to the polar coordinates of the point of observation. The total field distribution was a superposition of individually launched plasmons propagating toward/away the center, where the upper and lower limits of each integral indicated the boundary of the launched SPPs, defined by the TM-polarized sectors. Individual plasmon waves are described as planar waves (Eq. (2) with the attenuation term α and propagating constant β given by real and imaginary parts of $k_{SP} = k_0 [\varepsilon_d \varepsilon_m / (\varepsilon_d + \varepsilon_m)]^{1/2}$, where L is the radius of the virtual annular ring and ϕ_0 is the original point of the plasmon wave. The development of this equation was an extension of the interference model of two counter-propagating surface plasmon waves in the Kretchmann configuration [35]. Compared to FDTD method, this model did not provide an analytical solution to the formation of SPPs. Nevertheless, the discussion provided guidance for a qualitatively study of the field distribution of SPPs, when propagation behavior and interference were simultaneously affecting the results. In addition, the proposed phenomenological model provided a quick method to initiate a new design for SIP beams.

3. Simulation results

3.1 Single excitation of SPPs

To calculate the formation of SPPs, we imported the field distribution of focus, generated by vectorial diffraction theory, into commercial FDTD software, SIM 3D_MAX, by MMResearch. The two-dimensional field distributions of |Ez| component are identical to the field distribution of excited SPPs. Figure 3 illustrates the field distribution of excited SPPs for single excitation. To improve the visualization of the outer ring, the results were selected to illustrate the amplitude of its field distribution rather than intensity. With a single excitation, we modulated the size and position of a single TM-polarized sector to observe the corresponding SPPs fields. As shown in Fig. 3(a) and (b), the center of the angle of TM-polarized sector, ϕ_0, determined the direction of propagation of the plasmonic waves. The size of the TM-polarized sector, δϕ, corresponded reciprocally to the excited area. Such plasmonic manipulations show potential as a new scheme, for achieving high throughput and coupling efficiency for the planar plasmonic waveguides or devices.

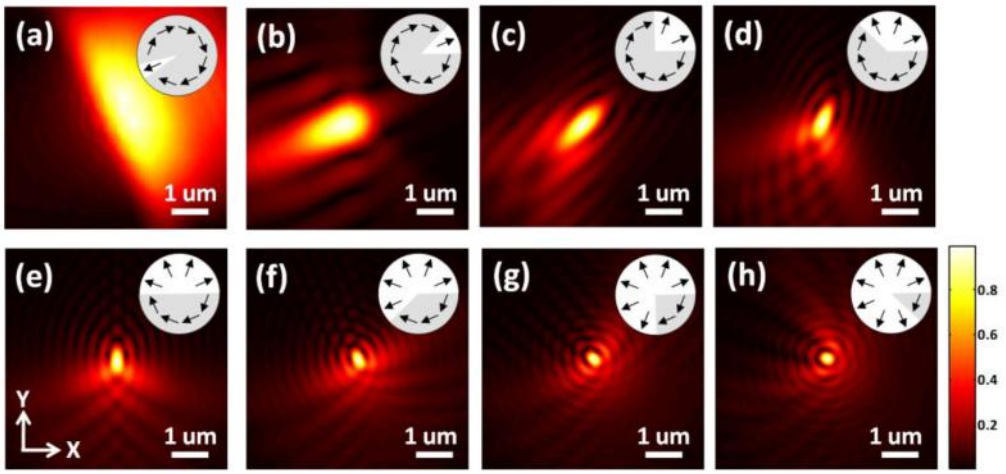

Fig. 3. The calculated field distribution of SPPs when the SIP beam was focused on the Au/Air interface. Subfigures (a) to (h) display single excitations with different ratios of TM-polarization (indicated with black arrows along the radial direction, indicated by the white background) at the pupil entrance, where (a) $\phi_0 = 202.5°$ and $\delta\phi = 22.5°$, (b) $\phi_0 = 22.5°$ and $\delta\phi = 45°$, (c) $\phi_0 = 90°$ and $\delta\phi = 45°$, (d) $\phi_0 = 67.5°$ and $\delta\phi = 135°$, (e) $\phi_0 = 90°$ and $\delta\phi = 180°$, (f) $\phi_0 = 112.5°$ and $\delta\phi = 225°$, (g) $\phi_0 = 135°$ and $\delta\phi = 270°$, (h) $\phi_0 = 157.5°$ and $\delta\phi = 315°$.

The field distribution of excited surface plasmon waves along the radial direction was expressed as $E_{SP} \sim E_0 \exp(ik_{sp}r)\exp(-L_{SP}/r)$, where L_{SP} was the propagation length with 1/e

#133327 - $15.00 USD Received 18 Aug 2010; revised 4 Oct 2010; accepted 13 Oct 2010; published 20 Oct 2010

attenuation of the SPPs amplitude and r represented the radial propagation distance from the position of excitation. The propagation constant and length of SPPs were calculated by taking the real part on the field distribution of |Ez|. In the case of $\phi_0 = 22.5°$ and $\delta\phi = 45°$ [Fig. 3(b)], the numerical result of the length of propagation and resonant wavelength were $L_{SP} = 0.98$ um and $\lambda_{SPP} = 601$nm, respectively. The numerical results agreed closely with the theoretical prediction under $\lambda_{SPP} = 2\pi/\mathrm{Re}[k_0(\varepsilon_1\varepsilon_2/\varepsilon_1 + \varepsilon_2)^{1/2}] = 598$ nm, whereas the theoretical length of propagation (6.24 um) was longer than that of the numerical results. This was because the field distribution of SPPs was formed by constructive interference induced from partially in-phase angular vector k_{sp}. This intensity peak was much higher than that of any ray excited surface plasmon wave.

When the size of the TM-polarized sector $\delta\phi$ was increased from 90° to 315°, the field distribution of excited SPPs revealed a gradual tendency toward local concentration, as shown in Figs. 3(c) to (h). In addition to the concentration of energy, the propagating SPPs were steered counterclockwise as $\delta\phi$ increased. At the same time, a series of interference ripples along the azimuthal plane became noticeable, yielding side lobes in the shape of discontinued arcs, due to the consequences of omni-directional SPPs propagation. As TM-polarized light occupied the entire pupil of illumination, the Bessel field distribution became excited creating a tiny spot at the center dressing the side lobe with a concentric ring. This was consistent with results in previous studies [11,12,14].

3.2 SPPs interference of double excitation

Figure 4 shows two animations of SPPs with different formations generated by the double excitation scheme. The polarization distribution of the SIP beam was designed to aid in the investigation of the interference behavior of the two propagated surface plasmons. In Fig. 4(a) (left side), the TM-polarized sector was divided into two equal parts where $\delta\phi = 45°$ and varied in $\Delta\phi$. The inserted TE-polarized sector acted as a barrier to isolate two generated plasmon waves with an angular distance $\Delta\phi$. As $\Delta\phi$ changed from 0 to 270 degree, the interferometric patterns of the two oblique plasmonic waves gained additional outer edges with corresponding sway. The angular distance between the two edges was identical to $\Delta\phi$. In addition, a constructive bright spot was observed at the center, which had been created by in-phase counter-propagating vectors, but was irrelevant to the change of angular distance.

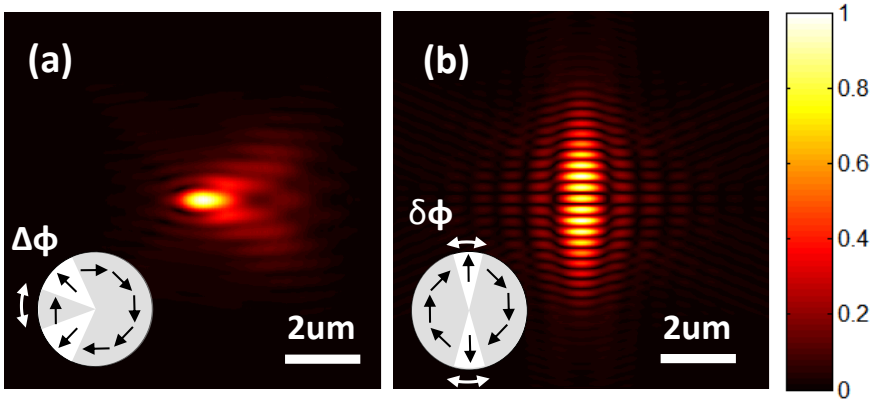

Fig. 4. A (left) (2.93 MB Media 1), b(right) (791 KB Media 2) two animations of field distribution for double excited SPPs generated by purposely designed SIP beams, with the point of observation lying on the plane of focus. (a) the TM-polarized sector is divided into two part with equal $\delta\phi$ but varied in $\Delta\phi$. As $\Delta\phi$ changed from 0° to 270°, the interferometric patterns of two oblique plasmonic waves show additional outer swayed edges. (b) the polarization distribution of SIP beam consists of double TM-polarized sectors which was arranged on the opposite side with variations in the size of $\delta\phi$. A clear plasmonic interference pattern spreading along vertical direction can be observed due to the counterpropagation of the SPPs.

#133327 - $15.00 USD Received 18 Aug 2010; revised 4 Oct 2010; accepted 13 Oct 2010; published 20 Oct 2010

Figure 4(b) (right side) depicts the normalized field distribution of SPPs observed on the focal plane illuminated by an SIP beam featuring two counter TM-polarized sectors with varied δϕ. A clear plasmonic interference pattern extending vertically was observed, due to the counter-propagation of the SPPs. The modulation of the interference pattern implied a recipitical relation between the size of sector and the lateral elongation of the interference lines. When the size of the sector δϕ shrank to a narrow slit on each side, the interference pattern of SPPs resembled that of two counter-propagating plane waves. This approach provided an easy, but effective way for scientists to investigate the interference of SPPs without the need for complicated nano-structures in the near-field.

3.3 Multiple excitations of SPPs with defocus

Figure 5 shows additional methods for the manipulation of the SPPs, via scanning the observation plane through the geometrical focus. As mentioned before, the cross-sectional points between every TM-polarized ray and dielectric/metal interface comprised a virtual annular ring referring to the initiation points of the SPPs. When metallic film was placed below (Z < 0) or over the focus (Z > 0), excited plasmonic waves propagated either toward the center or away from the virtual annular ring, yielding obvious or obscure individual interference patterns. One point of note was that the excitation position of SPPs shifted with additional extension or reduction, depending on the axial position of the focus, as shown in Fig. 5(a). This behavior was consistent with predictions from proposed phenomenological model. The radius of the virtual annular ring (the parameter of L in Eq. (3) was largely dependent on defocus.

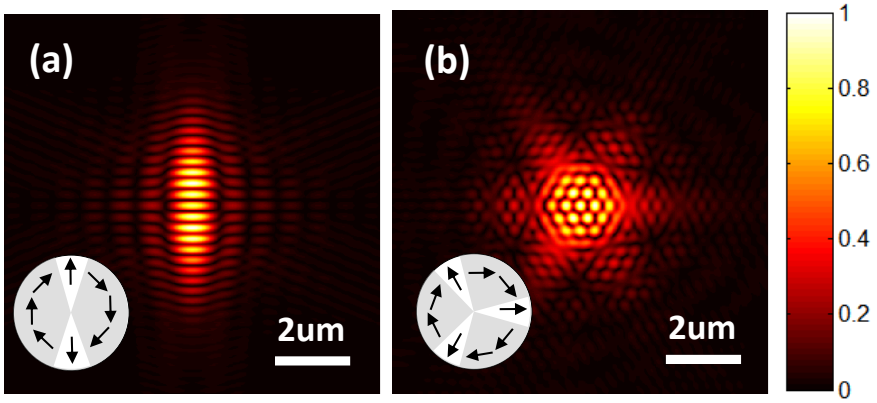

Fig. 5. a(left) (1.69 MB Media 3), b(right) (3.08 MB Media 4) two animations of field distribution for dual excited SPPs, generated by purposely designed SIP beams with the observation plane scanning through the focus. Movie a and movie b shows the field distribution of SPPs under specific SIP illuminating with dual and triple TM-polarized sectors (with equal δϕ = 45°), respectively.

As we split the TM-polarized sector into three sections and scanned the metallic film through the focus, several unusual patterns were observed. These had been created either by interference between counter-propagating plasmons at the center, or three independent propagating SPPs, as shown in Fig. 5(b). It is vital to note that the resulting interference patterns for such triple excitations was a group of 150-nm-radius (in magnitude of 1/e decay) bright spots in a 300-nm-period hexagonal arrangement caused by many in-phase SPPs. The separation distance and spot radii followed the basic concept of interference in which the period and the size are close to half the effective wavelength of SPPs. The spatial distribution of subwavelength spots could be manipulated by varying the size of individual TM-polarized sectors and the angular distance between each sector. On the other hand, when the focus moved above the interface, three propagated SPPs were simultaneously launched. This

#133327 - $15.00 USD Received 18 Aug 2010; revised 4 Oct 2010; accepted 13 Oct 2010; published 20 Oct 2010

yielded a field distribution in the shape of a shamrock. Such multiple excitations could be applied to future's applications in planner optics.

4. Experimental results

In order to validate the proposed scheme of single, double and triple excitations, we performed scanning near-field optical microscopy (SNOM) to produce a series of images of SPP distribution, utilizing an aperture-less fiber with a 50 nm diameter. This ensures tip collected information is proportional to the square modulus of the electric near field [36]. For simplicity, we used an apodized mask in place of the TE-polarized sector to imitate the spatial inhomogeneous polarized (SIP) beams. Figure 6 shows a comparison of two-dimensional intensity distribution of SPPs between experiments (a) – (e) and (f) – (j) simulation results. Figure 6(a) illustrates the single excitation scheme with $\delta\phi = 45°$, the projected SIP beam on focus forming an asymmetric SPP fields with Lsp = 1.38 um. This is in close agreement with corresponding simulation results in Fig. 6(f). For double excitation with a pair of opposite TM-polarized sectors ($\Delta\phi = 135°$ and $\delta\phi = 15°$) shown in Fig. 6(b), a series of straight parallel lines can be observed with 275 nm in period, which matched well with the simulated value of 273 nm. Based on this double excitation scheme using an arbitrary combination of size and angular distance of the TM-polarized pair, a variety of SPP patterns could be obtained from the complex combination of propagation behavior and interference effects, as shown in Fig. 6(c) where $\Delta\phi = 45°$ and $\delta\phi = 45°$. If we introduced additional 180° phase retardation in one sector, the central area of the fork would vanish, due to destructive interference of the counter-propagating SPPs. Another engineering factor would be the adjustment of the axial position of focus. When we split the pupil into three TM-polarized sectors and scanned the metallic film through the focus (z = –0.75 um, + 1 um), two things could be demonstrated. One was the arrangement of subwavelength spots into a hexagonal array; and the other was triple, simultaneously casted, surface plasmon waves, as shown in Fig. 6(d) and 6(e), respectively. Such self-interference patterns and multiple SPP steering could potentially be used to exposure photonic crystal in lithographic applications and to trigger multiple plasmonic sources for planar optics.

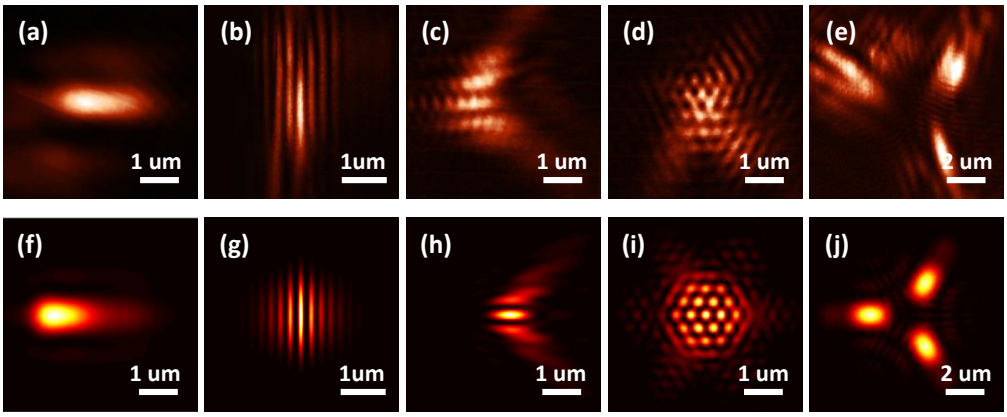

Fig. 6. A comparison of two-dimensional intensity distribution of SPPs between (a) – (e) experimental and (f) – (j) simulation results, where (a) single excitation with $\delta\phi = 45°$, (b) double excitation with $\Delta\phi = 135°$ and $\delta\phi = 15°$, (c) double excitation with $\Delta\phi = 45°$ and $\delta\phi = 45°$, (d) triple excitation with $\Delta\phi = 75°$, $\delta\phi = 45°$, and z = –0.75 um, and (e) triple excitation with $\Delta\phi = 75°$, $\delta\phi = 45°$, and z = + 1 um.

5. Conclusions

In summary, we proposed a novel scheme based on collinear configuration, in which we applied spatially inhomogeneous polarized light as a new illumination source to manipulate

#133327 - $15.00 USD Received 18 Aug 2010; revised 4 Oct 2010; accepted 13 Oct 2010; published 20 Oct 2010

the position of SPP excitation. We provided a phenomenological model to illustrate the generation mechanism and the underlying physics of the resulting field distribution. By designating combinations of size and angular distance of TM-polarized sectors on the pupil plane, we were able to verify a variety of SPP patterns through numerical calculation and experimental observation. These defocus techniques were also combined to switch the field distribution of SPPs, either in interference patterns caused by counter-propagating SPPs or simultaneously generated SPPs. The far-field approach offered a simple but effective means to steer SPPs and shape them on a metal surface, without the need for additional nano-structural features. Furthermore, this SPPs generator can provide time-dependent control as integrated with liquid crystal device for transforming conventional polarization into specific SIP beam. This method has definite potential in lithographic applications, plasmonic waveguides, and biophotonic devices.

Acknowledgement

The authors thank Chen-Yeh Ho for helpful discussions and experimental support. The financial support from National Science Council, Taiwan, under contract NSC 99-2221-E-009-067-MY3 is also acknowledged.

#133327 - $15.00 USD Received 18 Aug 2010; revised 4 Oct 2010; accepted 13 Oct 2010; published 20 Oct 2010